Progress In Electromagnetics Research C, Vol. 80, 199–209, 2018

Feasibility Study of Frequency Selective Surfaces for Structural Health Monitoring System

Syaiful Anas Suhaimi, Saidatul Norlyana Azemi*, and Ping Jack Soh

Abstract—A new type of three-dimensional (3D) Frequency Selective Surfaces (FSS) applied to passive sensing in Structural Health Monitoring (SHM) is presented. Such passive FSS sensors are proposed as an alternative to conventional sensors to eliminate the need of DC/AC power. Moreover, these FSSs are modified in a 3D form to feature enhanced performance compared to conventional FSSs and sensors. More specifically, the proposed 3D FSS is able to control its sensitivity $|S_{21}|$ in either TE or TM incident waves. In this project, incident angle characteristics are evaluated for SHM applications to obtain angular responses of up to 80 degrees. The resonant behavior of the TE-incident wave is shown to be sensitive towards the incident angle and is suitable to be used for monitoring any building tilting and damage. This is due to the significant 3D length changes of the conductor elements. Meanwhile, the TM-incident wave is found to be insensitive towards the incident angle.

1. INTRODUCTION

In recent years, Structural Health Monitoring (SHM) for infrastructures and buildings has attracted research attention. Its main aim is to ensure public safety by alerting stakeholders such as building and maintenance services for coming structural failures or health uncertainty caused by natural disasters. Moreover, SHMs are also capable of monitoring structural changes and stress before it reaches a critical condition, especially when high-rise accommodations are built in disaster-prone areas. Without early warning systems such as SHM, fatalities resulting from unexpected natural disasters or poor maintenance could be massive.

Various kinds of active sensors are already in use for SHM purposes. An example is the Radio Frequency Identification (RFID) tags, which were demonstrated to be capable of measuring the internal structure of concrete-covered materials for any loading capacity [1]. Besides concrete, such sensors are also suitable for monitoring structures made from other materials with less power consumption. Despite requiring less maintenance with high monitoring stability, the installation of these tags for detecting any strain is complicated and requires on-sensor battery power source. Wireless Sensor Networks (WSN) based on ZigBee technology is also used for monitoring the structural health of bridges, roads and buildings [2]. The advantages of this technology include low power consumption, good accuracy and reliability. Despite its advantages, Zigbee-based systems still require a huge number of active elements, which increases design and installation complexities. Meanwhile, the Acoustic Emission (AE) technology uses pressure waves which follow micro structural changes arising from the rapid output of strain energy in materials [3] and are popular in the monitoring of bridges made from steel and concrete [4]. AE is known for its robust elements and cost-effective installation. Unfortunately, such sensors are more environment-dependent, often noisy and produce weak signals. On the other hand, Optic Fiber Sensors (OFS) are suitable for SHM requirements, especially in the oil and gas industry sector for

Received 18 August 2017, Accepted 18 October 2017, Scheduled 22 January 2018
* Corresponding author: Saidatul Norlyana Azemi (snorlyana@unimap.edu.my).
The authors are with the Advanced Communication Engineering (ACE) CoE, School of Computer & Communication Eng., Universiti Malaysia Perlis, Arau, Perlis 02600, Malaysia.

monitoring buildings, bridges and roads [5]. This technology is passive and features low losses, no electrical interference and long distance measurement capability. However, fiber optics is very costly as it requires professional expertise for its complex installation and maintenance to attach or embed OFS inside building materials.

Recently, passive FSS was also applied in an SHM application. The 2D FSS sensors were bonded to the surfaces of existing structures for the detection and monitoring of strain and buckling displacement due to loading [6] using a combination of Microelectromechanical system (MEMS) and FSS [7]. Embedded between two surfaces, the FSS spacing is reduced when material between it compresses the FSS, resulting in a frequency shift. However, the combined use of MEMS and FSS resulted in a more complex design and foreseen complicated maintenance. Another FSS which acts as a wireless passive sensor for SHM and a chemical sensor in harsh environments has also been reported in [8]. Strain changes were detected by the re-radiated electromagnetic wave from the cross dipole FSS elements. Two polarizations (horizontal and vertical) were used to determine structural abnormalities using the FSS. However, this system is limited to detecting only horizontal cracks due to the insignificant electromagnetic wave changes resulting from the vertical cracks. The sensitivity of the angular response was improved in the passive FSS sensor proposed in [9]. However, the thickness-dependence of the proposed FSS adds to the fabrication complexity.

In this paper, an FSS is implemented in 3D form and applied to SHM to track and wirelessly monitor structure tilt without the need for any active components. Such a structure provides additional advantage over conventional 2D FSS in governing frequency response [10]. In contrast, 2D FSS are incapable of control over incident polarization angle due to its reduced sensitivity towards angular response. The building tilt angle can be more effectively monitored when it is sensitive to a single-polarized incident wave. This ideally requires either the TE- or TM-incident waves to cause a gradual shift of resonance frequency with the changes of building tilt angle. The orthogonal polarized wave, on the other hand, should be insensitive to these changes in the incident angles, indicating minimal resonance shifts with the incident angle variation, see Figure 1. To the best of the authors' knowledge,

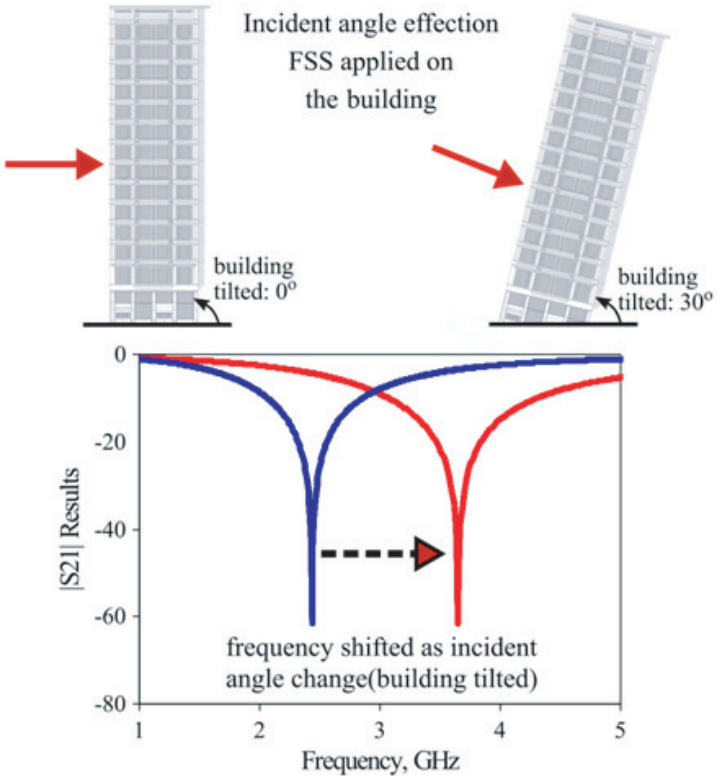

Figure 1. The concept of the FSS based wireless structural health monitoring.

such 3D FSS is proposed for the first time in open literature. Besides presenting a novel structure with improved sensitivity in comparison to an initial work in [9], a new pragmatic design equation for such structure is also presented in this manuscript.

The rest of the manuscript is organized as follows. The next section presents a 2D FSS design and demonstrates its limitation in SHM. This structure is then modified in Section 3 into a 3D form by elevating the height of the conductor cross sections. This structure is studied parametrically and experimentally relative to the incident angle (up to 80°) to validate its capability in detecting the changes in resonant frequency, prior to the conclusion in the final section.

2. TWO DIMENSIONAL (2D) FSS

The conducting elements of the 2D square loop FSS, which is the basis of this investigation, is formed on top of a 20 mm polystyrene substrate approximated as air. Despite numerous conventional FSS topologies proposed such as hexagonal [11], circular [12] and fractal [13], the choice of the square shaped FSS shown in Figure 2(a) offers modeling simplicity and improved performance especially in terms of stability of incident angle [14–16]. The square FSS is considered stable when its operating frequency does not change despite the variation in incoming wave angles. The optimization of the 2D FSS is performed by examining its various parameters such as the unit cell size, height of the conductor elements, h and the side length of the square, d, which is approximated as $d \approx \lambda/4$. The width, w of ($d2-d1 = 25.4$ mm–23.8 mm) governs the center resonant frequency, whereas the unit cell size influences the sensitivity of angular responses towards the incident angle of incoming waves. In short, the smaller dimension of d increases the resonant frequency, while the smaller unit cell dimension s enables more distinct angular responses.

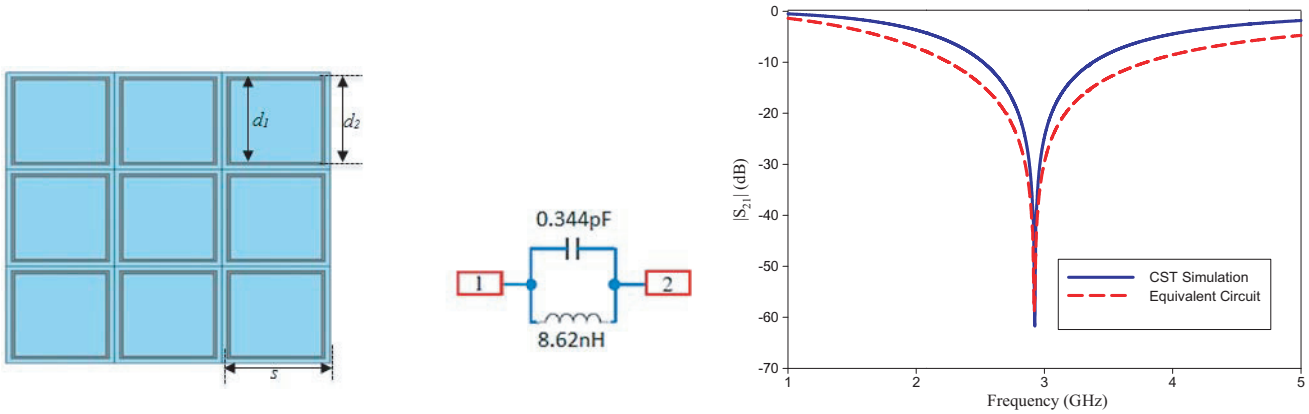

(a) (b) (c)

Figure 2. 2D square FSS design, (a) 3×3 unit cell square FSS, (b) equivalent circuit of the square FSS for one unit cell, (c) Square FSS $|S_{21}|$ result, CST Simulation vs Equivalent circuit.

An equivalent circuit of the 2D FSS shown in Figure 2(b) consisting of inductive and capacitive components in parallel was modeled to simplify the resonance estimation and analysis [17–19]. The simulated frequency response of the 2D square FSS shown in Figure 2(c) indicated a band stop response centered at 2.922 GHz. Resonant frequencies from the full-wave simulation and equivalent circuit model are compared to obtain the exact values for L_1 and C_1. The equations for the inductance and capacitance are as follows [20]:

$$L\,(\text{nH}) = 0.3937 \times 1^{-3} \left[\frac{\left(\frac{d_2 + d_1}{4}\right)}{8\left(\frac{d_2 + d_1}{4}\right) + 11\left(\frac{d_2 + d_1}{2}\right)} \right] \times \text{kg} \tag{1}$$

$$\text{kg} = 0.57 - 0.145 \ln \frac{w}{h}, \quad \text{if} \quad \frac{w}{h} > 0.05$$
$$C(\text{pF}) = \frac{1}{(2\pi f)^2 L} \tag{2}$$

In this investigation, five incident angles between 0° and 80° were studied to demonstrate the FSS sensing mechanism of the changes in incident angles. In the context of SHM, the deviation in tilt angle of the structure is expected to shift its frequency response. Figure 3 shows an example of two different sets of results by TE and TM incidences. The TE incident angles result indicated stable frequency response in two separate bands: 0° to 20° and 40° up to 80°. On the contrary, there exist set of irregular responses between 21° and 39°. Meanwhile, TM incident angle variation resulted in an upwards resonance shift. Due to its inconsistent performance for both TE and TM, it is deemed unsuitable for use as sensor for a SHM system.

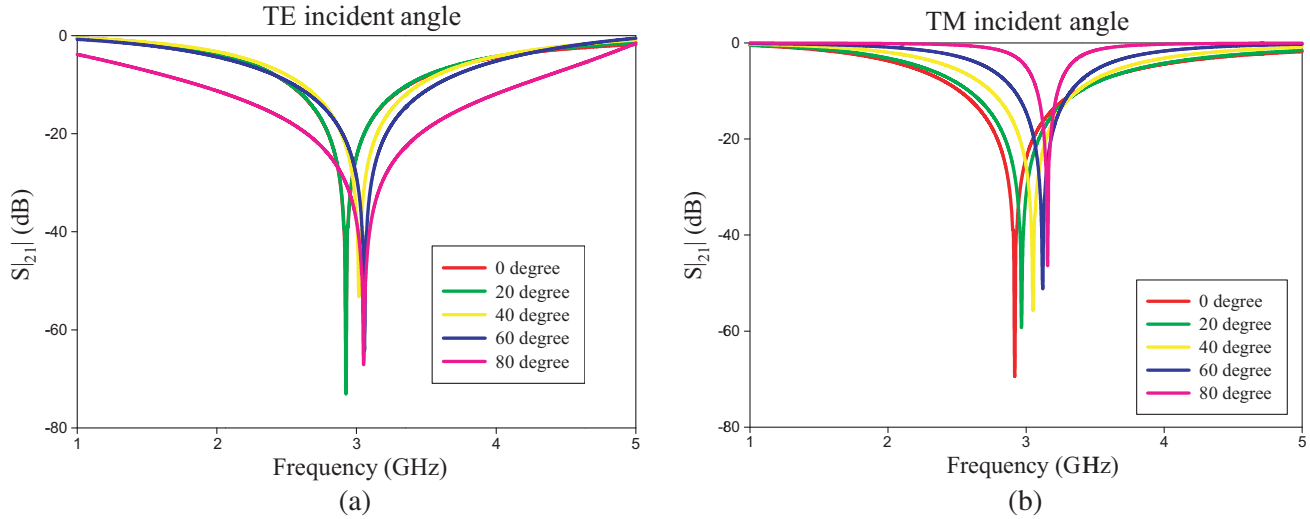

Figure 3. (a) $|S_{21}|$ for the 2D Square FSS with its incident angle varied from 0° to 80° (TE incident), (b) $|S_{21}|$ for the 2D Square FSS with its incident angle varied from 0° to 80° (TM incident).

The resonance of the 2D FSS is shown to vary as the incidence angle changes for TE and TM polarizations. When a signal is incident at an oblique angle on the FSS, in which conducting elements are separated by a width wc, the projected separation between the conducting elements (unit cell) will be reduced by a factor of $\cos\theta$, see Figure 4. When the incident angle becomes oblique, the induced current on the conductor elements are distinct, which means its higher intensity resulting in a varying FSS angular response [20]. In general, both TE and TM incident waves are sensitive to the incident angle, see Figure 3. However, the TE incident wave is less sensitive compared to TM incident waves, where the variations for the former is smaller compared to the latter. This is due to the similarity of polarization between the electric field of a TE incident wave and the direction of the conductor elements shown in Figure 5(a). These E-fields are also induced along its full parallel conductor dimension irrespective of incident angle, hence maintaining the same resonant frequency despite the changing incident angles. Meanwhile, for the TM incident waves shown in Figure 5(b), its E Field is oblique on the conducting element and results in incident angles increasing (and consequently frequency response shifting) despite the shorter projected conducting element lengths.

3. THREE DIMENSIONAL (3D) SQUARE FSS

Despite indicating some variation in terms of TM incident angles, the 2D FSS angular response sensitivity is insufficient for effective monitoring in SHM application. This is due to the sensitivity of such 2D FSS structures to both TE- and TM-incident waves. In contrast, the building tilt angle

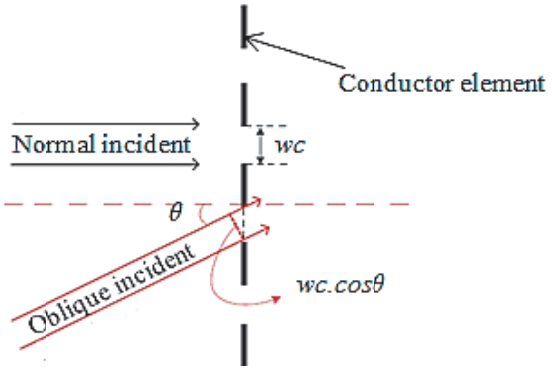

Figure 4. Separation between the unit cells incident angle.

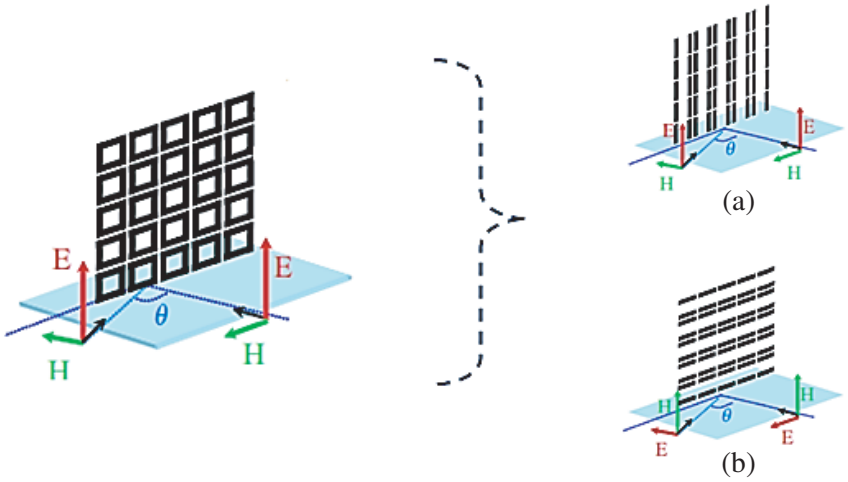

Figure 5. Different signal polarization incident on the conducting elements of the square ring FSS, (a) TE incidence waves, (b) TM incidence waves [21].

can be more effectively monitored when it is sensitive to only a single-polarized incident wave, either the TE- or TM-incident waves. To overcome this limitation and enhancing angular response sensitivity, a 3D FSS is introduced. This structure is a modification of the proposed 2D FSS by protruding the conductor's height. Using the same simulator, the 3D square FSS was designed and simulated using various structural geometries. The dimension of the 3D square FSS substrate, s is 28 mm and the side length of the square, d is 25.4 mm. The height, h of the 3D FSS was optimized from 0.035 mm to 18 mm while keeping its diameter and unit cell size constant. A basic equation is derived to design 3D FSS with normal incidence (0°) at a frequency 4.3 GHz with $d = 25.4$ mm and $h = 18$ mm, in terms of wavelength $\lambda/3$ and $\lambda/4$ respectively, as follows.

$$\begin{aligned} \text{where, } \lambda &= 3d \text{ and } \lambda = 4h \\ c &= \text{ speed of light } (3 \times 10^8 \text{ m/s}) \\ \text{Therefore: } f &= \frac{c}{3d}, \quad f = \frac{c}{4h} \text{ at 0 angle for TE and TM resonant} \\ d &= \frac{4h}{3}, \quad h = \frac{3d}{4} \end{aligned} \tag{3}$$

The 3D FSS composed of metallic squares exhibits a resonant behavior described by an LC circuit shown in Figure 6. For cylinders with length of $l \approx 0$, the square FSS exhibits a band-stop response, resonating at a frequency of $f = 1/(2\pi\sqrt{L_1 C_1})$, where L_1 and C_1 are the equivalent inductance and capacitance of the circular ring geometry. The diameter of the ring, d mainly also influences L_1 and

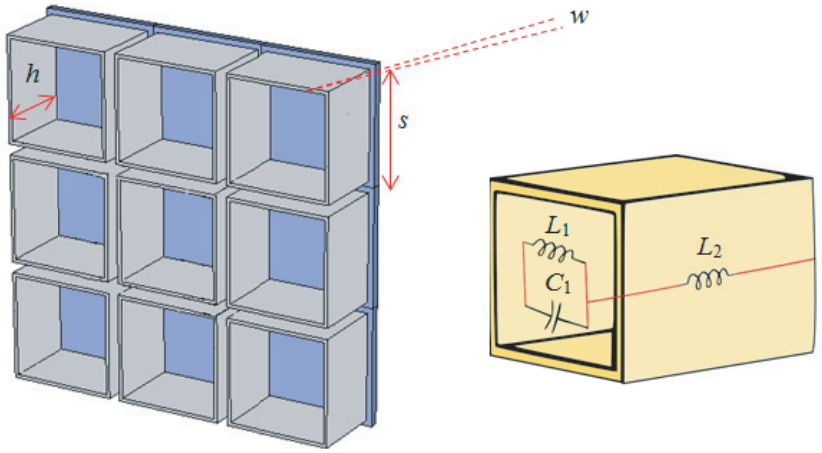

Figure 6. 3D square FSS dimension and its equivalent circuit model.

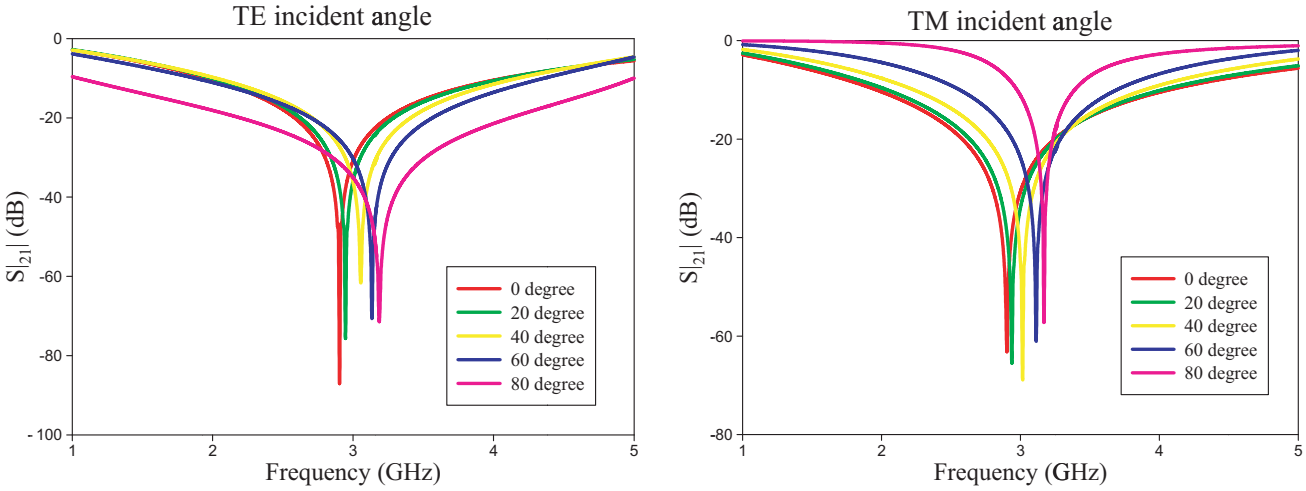

(a) TE and TM incidence waves at a height of 5mm

consequently the element's resonant frequency. As this 3D square-shaped structure performs similarly to a cylindrical 3D FSS [22, 23], the elevation of the FSS conductor height (from 2D to 3D) results in an increase of L_2 and changes the angular response behavior [23].

Figure 7 shows the frequency response of the 3D FSS. Significant rate of change can be observed in resonance upon incident angle variations upon the height increment of the FSS conducting elements from 2D to 3D. The TM incident waves became more stable (insensitive) while TE incident waves became sensitive towards angular response. This behavior indicates that the height of the conductor elements influenced the characteristic of the 3D FSS. As illustrated in Figure 7, the results at a height 18 mm for TM incident waves are stable, while the TE incident waves are angle-sensitive. This allows for its effective function as passive sensors for SHM application.

Figure 8 illustrates the surface current density of the 3D FSS element. It shows that its half mode at an element height of 18 mm resonates at 4.327 GHz. This half mode is identified based on the equation below [24]:

$$f_r = \frac{1}{2\sqrt{\mu\varepsilon}}\sqrt{\left[\left(\frac{m}{d_1}\right)^2 + \left(\frac{n}{d_1}\right)^2 + \left(\frac{p}{h}\right)^2\right]}\,(\text{GHz}) \tag{4}$$

The theoretical study of the FSS resonance indicates that there is a linear relationship between the change in incident angle and resonant frequency shift. This is validated further experimentally. Both

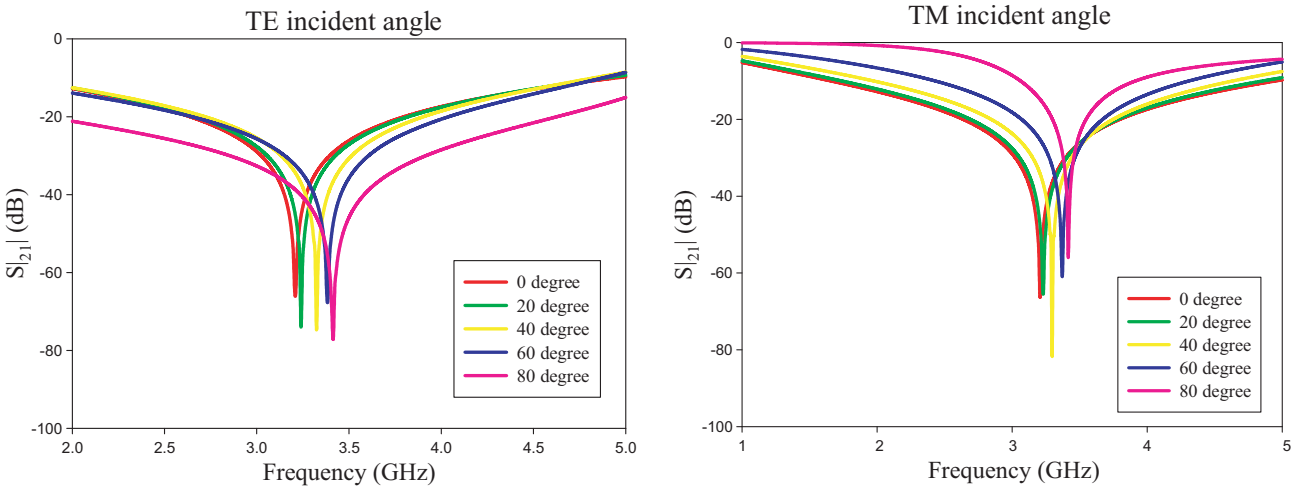

(b) TE and TM incidence waves at a height of 10 mm

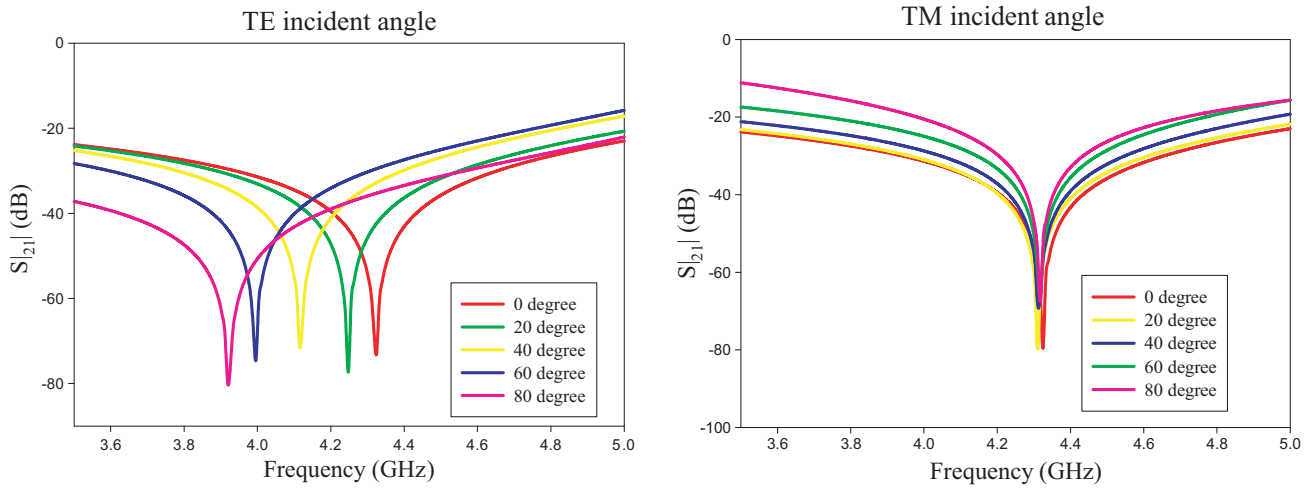

(c) TE and TM incidence waves at a height of 18mm

Figure 7. Simulation result for TE and TM incidents with FSS heights of (a) 5 mm, (b) 10 mm, (c) 18 mm.

3D FSS modeling and experiments show that the resonant frequency f_r, of the structure shifts to f_{rs} (shifted frequency) relative to the incident angle variation. Table 1 summarizes the measured deviation percentage, which indicates a good contrast in monitoring structural changes in SHM application. The theoretical relationship between the incident angle changes and the frequency shift is derived as follows:

$$\theta = \sin^{-1}\left[\frac{\left(\frac{\lambda_s - \lambda_o}{d}\right)t}{\lambda_o}\right] \tag{5}$$

$$\text{where; } d = 0.07 \times 10^{-3}, \quad t = 1.34 \times 10^{-3}$$

$$\text{and } \lambda_o = \frac{c}{f_r}, \quad \lambda_s = \frac{c}{f_{rs}}$$

where d is the angular difference between f_o and f_{rs} upon conversion in terms of wavelength while t is median average frequency deviation. The deviation is calculated after simulations and measurements have been conducted for angles up to 80°.

A 6×6 prototype of the 3D square FSS, each with a height 18 mm, was then fabricated using aluminum as shown in Figure 7(c) based on the model in Figure 9. It was measured using the free space measurement technique using two horn antennas. The setup was first calibrated using a flat metal plate

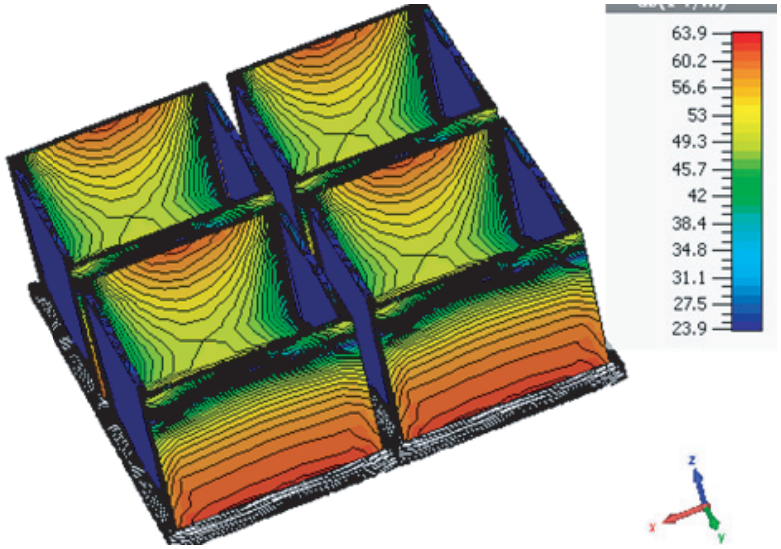

Figure 8. Surface current of 3D FSS in half wavelength.

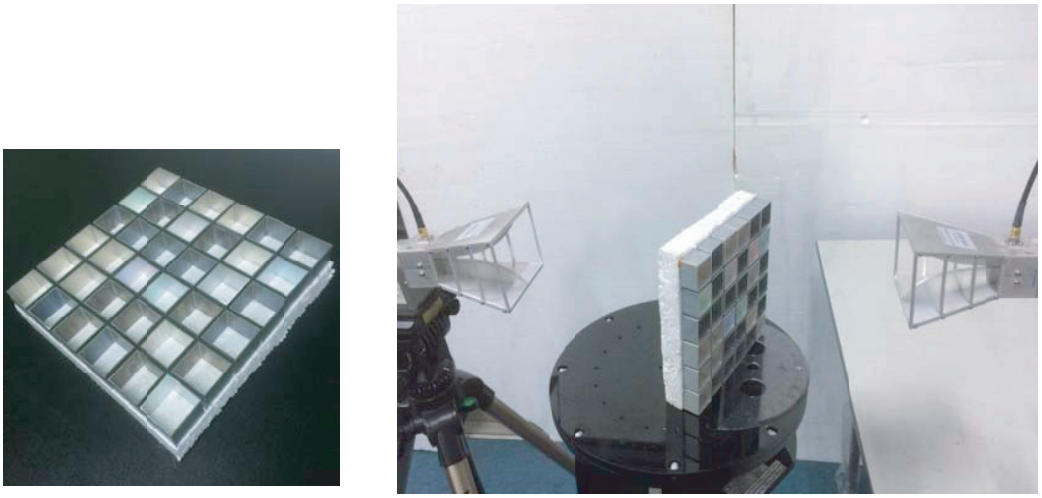

(a) (b)

Figure 9. (a) Prototype of 3D square FSS, (b) free space measurement setup with varied incident angle.

sized similarly with the FSS prototype. Next, this FSS prototype is then placed in between the two horns with a 10 cm distance from each horn before its transmission properties are measured.

The results of the TE and TM incident waves are then experimentally assessed from 0° up to 80° to mimic the tilted building scenario. The shift in the FSS resonant frequency is depicted in Figure 10, with an arrow indicating the direction of the downwards resonance shift. Approximately 0.18 GHz shift and 5% deviation is observed for every 20° of angle of incident variation.

Simulation and measurement comparison between TE and TM-polarized incident angles indicates satisfactory agreements. A small disagreement is observed between measured and simulated frequency responses with the angular variation for TE incident waves. Nonetheless, the TE frequency responses indicated the same downwards-shifting behavior, as predicted in simulations. On the other hand, the TM incidence wave is sensitive of the angular response. These simulation-measurement results and the contrast achieved by the deviation angle demonstrated the suitability of the 3D FSS for the SHM application.

Table 1. Measured centre frequencies of the 3D square FSS with different height.

height, $h = 18$ mm (TE incidence)		
Degree (°)	Frequency (GHz)	Deviation (%)
0	4.31	0
20	4.22	−0.28
40	4.13	−4.17
60	3.97	−7.88
80	3.75	−12.9

height, $h = 18$ mm (TM incidence)		
Degree (°)	Frequency (GHz)	Deviation (%)
0	4.29	0
20	4.28	−0.23
40	4.26	−0.69
60	4.3	−0.23
80	4.32	−0.69

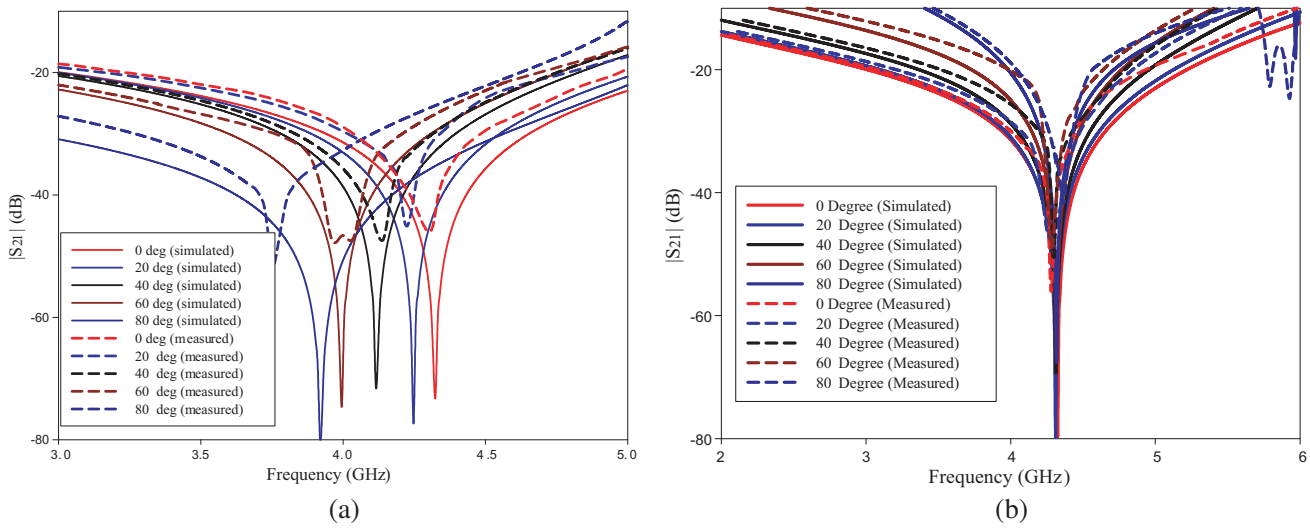

Figure 10. Measurement and simulation results of (a) TE incident angle and (b) TM incident angle.

4. CONCLUSION

In this paper, a new FSS technique applied in SHM is proposed and investigated. This 3D FSS acts as a passive sensor with increased sensitivity and in contrast to conventional 2D FSS for monitoring structural abnormalities in buildings. The conductor elements, studied at the optimized height of 18 mm in this case, subsequently enable the 3D FSS to obtain angular-dependent responses for the polarization of TE and TM incidences. Besides that, it is also demonstrated that there is a linear relationship between the incident angle and the frequency shifting, resulting in a novel design equation for such 3D FSS structures.

ACKNOWLEDGMENT

The authors would like to acknowledge the contributions of Mr. Herwansyah Lago for his technical contributions during the experimental validations.

This work was financially supported in part by the Fundamental Research Grant Scheme (FRGS) (under grant no: 9003- 00545) and the MyBrain Scholarship, both provided by the Malaysian Ministry of Higher Education (MoHE).

REFERENCES

1. Ikemoto, Y., S. Suzuki, H. Okamoto, H. Murakami, H. Asama, S. Morishita, T. Mishima, X. Lin, and H. Itoh, "Force sensor system for structural health monitoring using passive RFID tags," *2nd IEEE Int. Interdiscip. Conf. Portable Inf. Devices 2008 7th IEEE Conf. Polym. Adhes. Microelectron. Photonics*, Vol. 29, No. 2, 1–6, Garmish-Partenkirchen, 2008.
2. Jiang, X., Y. Tang, and Y. Lei, "Wireless sensor networks in structural health monitoring based on ZigBee technology," *3rd Int. Conf. Anti-counterfeiting, Secur. Identif. Commun.*, 449–452, 2009.
3. Tan, A. C., M. Kaphle, and D. Thambiratnam, "Structural health monitoring of bridges using acoustic emission technology," *2009 8th Int. Conf. Reliab. Maintainab. Saf.*, No. C, 839–843, 2009.
4. Lovejoy, S. C., "Acoustic emission testing of beams to simulate SHM of vintage reinforced concrete deck girder highway bridges," *Struct. Heal. Monit.*, Vol. 7, No. 4, 329–346, 2008.
5. Lopez-Higuera, J. M., L. Rodriguez Cobo, A. Quintela Incera, and A. Cobo, "Fiber optic sensors in structural health monitoring," *J. Light. Technol.*, Vol. 29, No. 4, 587–608, 2011.
6. Pieper, D., K. M. Donnell, O. Abdelkarim, and M. A. ElGawady, "Embedded FSS sensing for structural health monitoring of bridge columns," *IEEE Int. Instrum. Meas. Technol. Conf. Proceeding*, 1–5, 2016.
7. Pavia, J. P., W. J. Otter, S. Lucyszyn, and M. A. Ribeiro, "Design of a THz-MEMS frequency selective surface for structural health monitoring, *International Conference on Meta*, 2016.
8. Jang, S.-D. and J. Kim, "Wireless structural sensor made with frequency selective surface antenna," *Proc. SPIE — Int. Soc. Opt. Eng.*, Vol. 8344, 1–7, 2012.
9. Suhaimi, S. A., S. N. Azemi, and S. P. Jack, "Structural health monitoring system using 3D frequency selective surface," *IEEE Asia-Pacific Conf. Appl. Electromagn.*, 145–149, 2016.
10. Azemi, S. N., K. Ghorbani, and W. S. T. Rowe, "3D frequency selective surfaces with wideband response," *Int. Work. Antenna Technol. Small Antennas, Nov. EM Struct. Mater. Appl. 2014*, 212–215, IEEE, 2014.
11. Zheng, S. F., Y. Z. Yin, H. L. Zheng, Z. Y. Liu, and A. F. Sun, "Convoluted and interdigitated hexagon loop unit cells for frequency selective surfaces," *Electron. Lett.*, Vol. 47, No. 4, 233, 2011.
12. Fauzi, N. A. M., M. Z. A. A. Aziz, M. A. M. Said, M. A. Othman, and B. H. Ahmad, "Investigation of impedance modeling for a unit cell of the circle loop frequency selective surface at 2.40 Hz," *IEEE Int. Conf. Control Syst. Comput. Eng.*, 28–30, Nov. 2014.
13. Ratnaratorn, C., C. Mahatthanajatuphat, and P. Akkaraekthalin, "Gain enhancement for multiband antenna with frequency selective fractal surface reflector," *Proc. Asia Pacific Microw. Conf. 2014*, Vol. 714–716, 6–8, 2014.
14. Lee, Y. S., F. Malek, and F. H. Wee, "Investigate FSS structure effect on WiFi signal," *5th IET Int. Conf. Wireless, Mob. Multimed. Networks (ICWMMN 2013)*, 331–334, Beijing, 2013.
15. Seman, F. C. and N. K. Khalid, "Investigations on fractal square loop FSS at oblique incidence for GSM applications," *2014 Electr. Power, Electron. Commun. Control. Informatics Semin. Investig.*, 62–66, 2014.
16. Aziz, M. Z. A. A., M. M. Shukor, B. H. Ahmad, M. K. Suaidi, M. F. Johar, M. A. Othman, S. N. Salleh, F. A. Azmin, and M. F. A. Malek, "Investigation of a square loop frequency selective surface (FSS) on hybrid material at 2.4 GHz," *Proc. — 2013 IEEE Int. Conf. Control Syst. Comput. Eng. ICCSCE*, 275–278, 2013.
17. Hong, J. and M. J. Lancaster, *Microstrip Filters for RF/Microwave*, Vol. 7, 2001.

18. Costa, F., A. Monorchio, and G. Manara, "An equivalent circuit model of frequency selective surfaces embedded within dielectric layers," *2009 IEEE Antennas Propag. Soc. Int. Symp. Charleston*, No. 1, 0–3, SC, 2009.
19. Ferreira, D., R. F. S. Caldeirinha, I. Cuiñas, and T. R. Fernandes, "Square loop and slot frequency selective surfaces study for equivalent circuit model optimization," *IEEE Trans. Antennas Propag.*, Vol. 63, No. 9, 3947–3955, 2015.
20. Sung, G. H., K. W. Sowerby, M. J. Neve, and A. G. Williamson, "Frequency-selective wall for interference reduction in wireless indoor environments," *IEEE Antennas Propag. Mag.*, Vol. 48, No. 5, 29–37, 2006.
21. Hamdy, S. and E. Parker, "Current distribution on the elements of a square loop frequency selective surface," *Electron. Lett.*, Vol. 18, No. 14, 624–626, 1982.
22. Azemi, S. N. and W. S. T. Rowe, "Development and analysis of 3D frequency selective surfaces," *2011 Asia-Pacific Microw. Conf. Proc.*, 693–696, 2011.
23. Azemi, S. N., K. Ghorbani, and W. S. T. Rowe, "3D frequency selective surface," *Progress In Electromagnetics Research C*, Vol. 29, 191–203, 2012.
24. Erdogan, L., C. Akyel, and F. M. Ghannouchi, "Dielectric properties of oil sands at 2.45 GHz determined by a rectangular cavity resonator," *J. Microw. Power Electromagn. Energy*, Vol. 45, No. 1, 15–23, 2011.